



# Splat Morphology and Influence of Feeding Rate During Reactive Plasma Spray of Aluminum Powder

Mohammed Shahien, Motohiro Yamada, and Masahiro Fukumoto

(Submitted February 2, 2016; in revised form April 17, 2016)

Fabrication of aluminum nitride (AlN) coatings using conventional plasma spraying processes directly has been deemed impossible. It is attributed to the thermal decomposition of the AlN feedstock particles during spraying without a stable melting phase. Using the reactivity of the plasma (reactive plasma spraying: RPS) showed a promising consideration for in situ formation of AlN thermally sprayed coatings. Several AlN-based coatings were fabricated through the RPS of aluminum powders in the  $N_2/H_2$  plasma. The focus of this study is in discussing the morphology of splat deposition during the nitriding of Al particles. Furthermore, the influence of the feeding rate during the RPS and nitriding of Al powders will be investigated. The nitride content, as well as the unreacted molten Al phase, strongly influences splat deposition and morphology during the RPS of Al. The collected splats can be divided into reacted, partially reacted, and unreacted splats. The reacted splats tend to show a disk or egg-shell shape. The partially reacted mainly had outside nitride shells and an unreacted molten Al part in the center. The unreacted splats tended to show a splash shape. The main controlling factor is the time of the droplet impact on the substrate during the reaction sequence. The particle size and spray distance showed significant effects on the splat formation due to their effect on the nitriding conversion and the melting behavior of the particles during RPS nitriding. The powder feeding rate was investigated through increasing the injection rate and by using a low carrier gas flow rate. Increasing the powder feeding rate significantly improved the coating thickness. However, it suppressed the nitriding conversion of the large Al particles. Thus, with increasing the amount of the powder in the plasma, the Al molten particles are easily aggregated and agglomerate together upon colliding on the substrate with an AlN shell on the surface. This prevents the  $N_2$  from having access to all of the aggregated particles. Therefore, the fabricated coatings using large Al particles consist of surface AlN layers and the central parts of AlN and Al composite layers. On the other hand, it was possible to fabricate about 500- $\mu\text{m}$ -thick AlN coatings using fine Al particles of 15  $\mu\text{m}$  and increasing the feeding rate. Using the fine particles improved the nitriding reaction due to the improvement of the surface area (the reaction area). Moreover, the nitriding process of the Al particles with increasing the feeding rate was also investigated.

**Keywords** aluminum powder, particle size, powder feeding rate, reactive plasma spray, splat morphology

## 1. Introduction

Thermal spraying is a versatile deposition technique of abrasion-resistant and protective coatings. The process is based on rapidly heating and accelerating a solid feedstock material at a high velocity by a hot gas, flame, or plasma jet. Then, the molten or semi-molten (heat softened) material is propelled onto a substrate surface and forms the coating. Although several feedstock materials such as metal, alloy, ceramics, polymer, or their composites in different forms (powder, wire, or rods) can be used in thermal spray process, it is however, difficult to deposit several refractory ceramic coatings such as aluminum nitride (AlN) by conventional thermal spray processes. This is attributed to the thermal decomposition of the feedstock AlN particles during spraying without a stable melting phase. Figure 1 shows the sample after the spraying of AlN powder using a conventional atmospheric plasma spraying system. It is clear that just few particles impinged on the substrate and that it is easy to remove them by scratching. AlN exhibits a unique combination of properties: high thermal conductivity, high electrical resistivity, high hardness, good

This article is an invited paper selected from presentations at the 7th Asian Thermal Spray Conference (ATSC 2015) and has been expanded from the original presentation. ATSC 2015 was held in Xi'an, China, during September 23–25, 2015, and was organized by the Asian Thermal Spray Society in association with Xi'an Jiaotong University, State Key Laboratory for Mechanical Behavior of Materials.

**Mohammed Shahien**, Toyohashi University of Technology, 1-1, Tempaku-cho, Toyohashi 441-8580, Japan and Advanced Materials Department, Central Metallurgical R& D Institute (CMRDI), Cairo, Egypt; and **Motohiro Yamada** and **Masahiro Fukumoto**, Toyohashi University of Technology, 1-1, Tempaku-cho, Toyohashi 441-8580, Japan. Contact e-mail: mo.shahien@yahoo.com.

corrosion resistance, wear resistance, and good chemical/physical stability (Ref 1-3). The AlN properties are promising for several electronic and electric applications.

Using the reactivity of the thermal plasma (reactive plasma spraying: RPS) is a promising solution for the fabrication of AlN thermal sprayed coatings. The process basically depends on the reaction of a molten feedstock, like aluminum (Al) particles, with the surrounding active nitrogen plasma. Then the particles collide and rapidly solidify on the substrate. It was possible to fabricate AlN nitride coatings through the nitriding of Al particles in a nitrogen radio-frequency (RF) plasma jet (Ref 4, 5). Furthermore, in our previous studies (Ref 6-16), it was possible to fabricate several AlN-based coatings through the RPS of different feedstock powders using the nitrogen-hydrogen plasma of an atmospheric DC plasma spraying system. The reactive plasma spraying of Al particles is strongly affected by the reaction-related parameters such as the reacting time, particle size, and chemical additives. However, there are a lot of aspects such as the splat morphology and the effect of the powder feeding rate during the RPS process which require further optimization for establishing the RPS process.

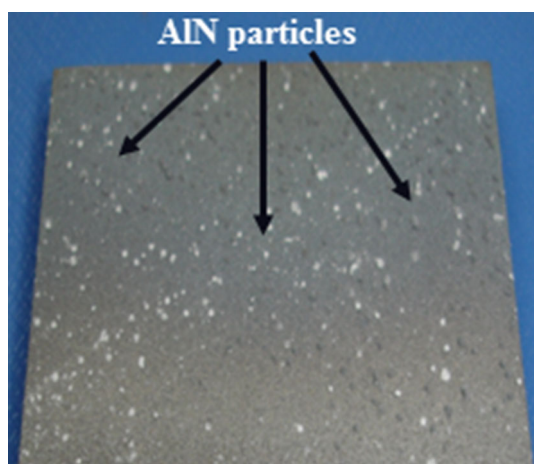


**Fig. 1** The sample after spraying AlN powder using Ar/H<sub>2</sub>, by conventional APS plasma spray process: APS: 9 MB, Sulzer Metco, Switzerland

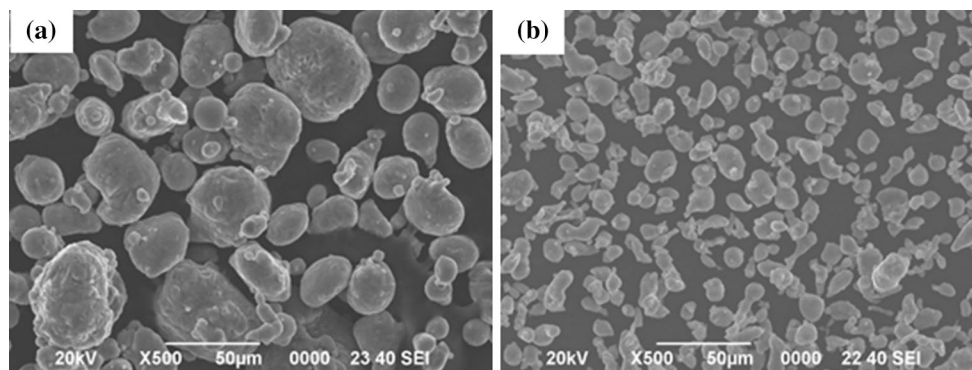


**Fig. 2** SEM morphology of the Al feedstock powders with average particle size: (a) 30 and (b) 15 μm

Thus, there are several studies investigating the splat formation and morphology in a conventional plasma spray process, and generally the splat can be simply categorized as disk splat or splash splat (Ref 17-19). In addition, during the RPS process, the chemical reaction and its related parameters had a significant effect on particle deposition and the coating formation process. Therefore, this study will focus on investigating the splat shape during the RPS process from the reaction point of view and consider the other splat controlling parameters to be constant.

On the other hand, the powder feeding rate is an important factor to adjust the coating process, the coatings microstructure, and properties in plasma spray process. As reported by Fauchais et al. (Ref 20-22), the powder feed rate and flowability must be controlled to make the spray process consistent and reproducible. In addition, in the RPS process, the feeding rate is expected to have a strong effect on the chemical reaction between the feedstock powder and the surrounding active gases in the plasma.

This study will clarify the splat morphology during the reactive plasma spraying and nitriding of Al particles. Furthermore, the influence of the powder feeding rate on the coating formation and coating microstructure during the RPS of Al will be experimentally investigated.

## 2. Experimental Procedure

Commercial pure aluminum powders (Toyo Aluminium K. K., Japan) with two different average particle sizes of 30 and 15 μm were used as starting feedstock powders. The morphology of the aluminum powders is shown in Fig. 2. The particles are quasi-spherical in shape. The particle size distributions and the typical contents of the feedstock Al powders (as received from the supplier) are shown in Table 1. All spraying experiments were carried out by a conventional atmospheric plasma spraying system (APS: 9MB, Sulzer Metco, Switzerland) as illustrated in Fig. 3. The system was modified as a reactive plasma spraying system for using N<sub>2</sub> as primary gas and H<sub>2</sub> as secondary gas. The process is based on the reaction between the Al particles and the surrounding active nitrogen and hydrogen species. The details of the system

and the RPS process have been reported previously (Ref 6-12). Table 2 shows the spray parameters used in this study. The spray distance (between the spray gun exit to the substrate surface) was kept at 100 or 150 mm.

For splat observation, a micro-feeder (FPS-Technoserve, Toyohashi, Japan) was used to supply the feedstock powder to the plasma stream. The Al particles were sprayed toward mirror-polished SUS304 substrate under the same experimental conditions which were used during the coating process. On the other hand, for the coating fabrication grid, blasted mild steel plates (50 mm × 50 mm × 5 mm) were prepared as the substrate material. During the splat collection, after setting the mirror-polished substrate, the traverse speed (scanning or coating speed) was increased from 30 mm/s (which is used for coating formation) to 150 mm/s. During the splat collection, the traverse speed was increased to avoid coating formation and to collect well-separated individual particles on the substrate for morphology observation. The traverse speed was then optimized to 150 mm/s.

The effect of the powder feeding rate during the reactive plasma spraying of Al powder was investigated by increasing the powder injection rate, using a standard

powder feeder (PL-10NS-Technoserve, Toyohashi, Japan) and while maintaining a constant carrier gas flow rate (1 L/min). Figure 4 shows a schematic diagram and the injection mechanisms for both the micro- and standard powder feeders. The micro-feeder is based on using a local fluidized bed feeding system and the standard powder feeder is based on a rotating wheel system.

The phase compositions of the coatings were verified by x-ray diffraction (XRD: RINT-2500, Rigaku, Tokyo, Japan) with CuK $\alpha$  radiation. The microstructure of the fabricated coatings' cross-section and the collected splats were observed using a scanning electron microscope (SEM: JSM-6390, JEOL, Tokyo, Japan). Elemental analysis of the fabricated coatings' cross-section was carried out by energy-dispersive x-ray (EDX; JSM-6300, JEOL, Tokyo, Japan).

### 3. Results and Discussion

#### 3.1 Splat Morphology During Reactive Plasma Spray Nitriding of Al Powders

The focus of this section is investigating the influence of the reactive plasma nitriding on the splat shape and with consideration that the other splat-related

**Table 1** The particle size distributions and typical contents of the Al powders

	Al 30	Al 50
D10, $\mu\text{m}$	19.77	8.46
D50, $\mu\text{m}$	35.08	15.38
D90, $\mu\text{m}$	62.82	27.77
Al, mass%	99.78	99.79
Fe, mass%	0.16	0.16
Cu, mass%	TR	TR
Si, mass%	0.06	0.05
Zn, mass%	TR	TR
Mn, mass%	TR	TR
Mg, mass%	TR	TR
Ti, mass%	TR	TR

**Table 2** The typical spray conditions

1st gas: pressure, kPa:flow rate, L/min	N <sub>2</sub> : 330.9:47.2
2nd gas: pressure, kPa:flow rate, L/min	H <sub>2</sub> : 344.7:2.3
Arc current, A	500
Arc voltage, V	70-80
Spray distance, mm	100-150
Carrier gas: flow rate, L/min	N <sub>2</sub> : 1
Substrate materials	SS400SUS304
Traverse speed, mm/s	
For splat collection	150
For coating deposition	30

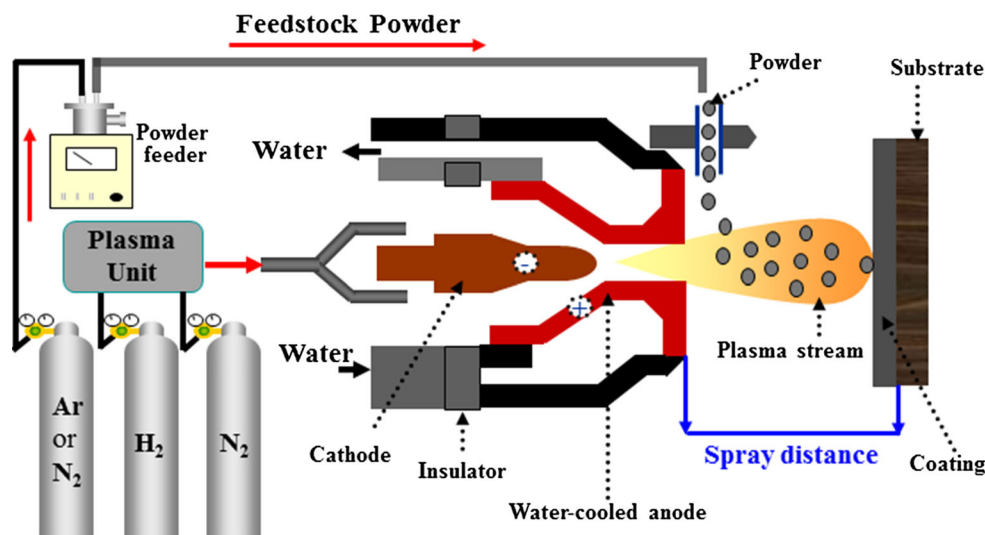


**Fig. 3** Schematic diagram of APS atmospheric plasma spray system

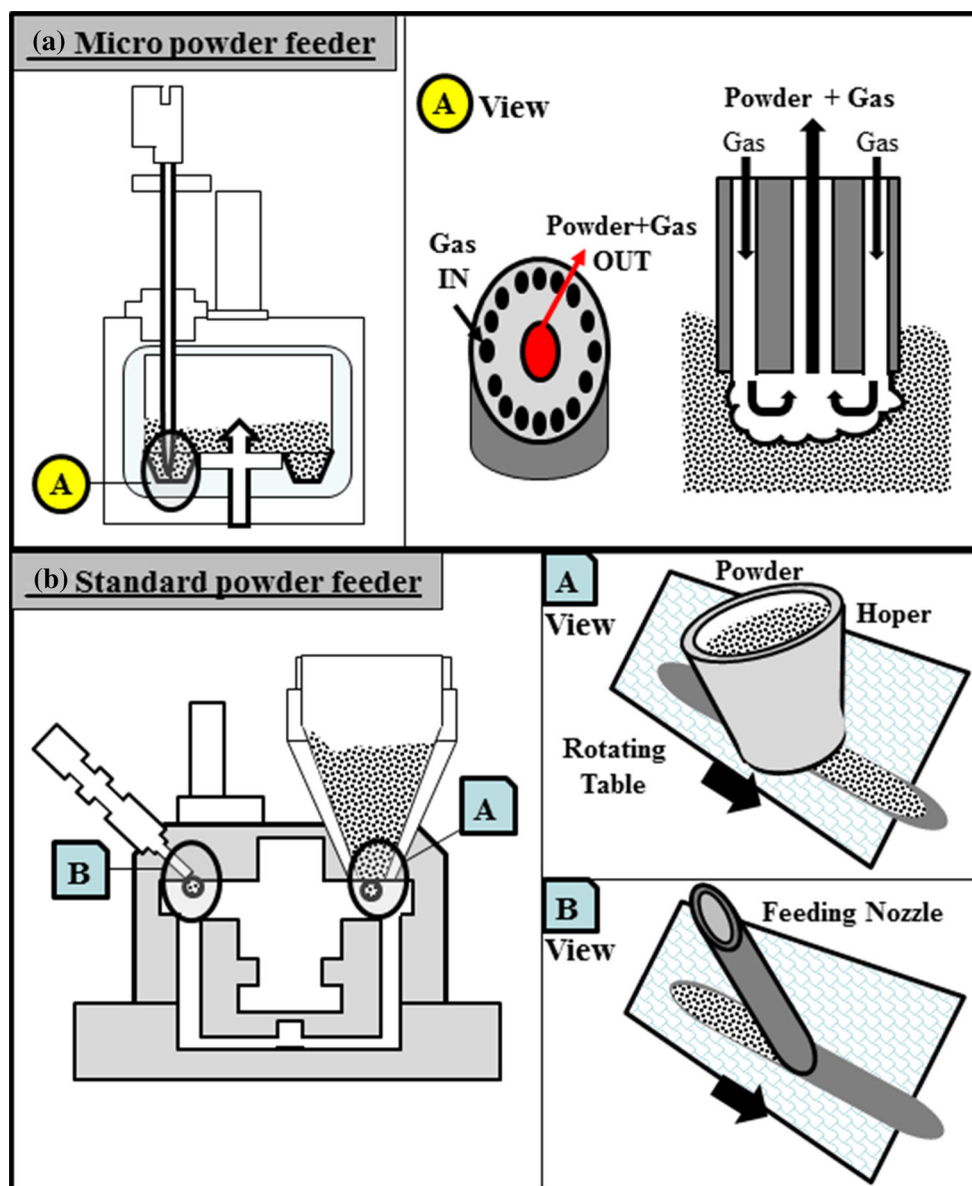


**Fig. 4** The schematic diagram and the injection mechanism for the micro- and standard powder feeders

parameters (substrate temperature, plasma power, substrate roughness, —) are constant. Figure 5 and 6 show the morphology of the collected droplets in case of 30- and 15- $\mu\text{m}$  Al powders, respectively. The collected droplets were divided into three groups: reacted, partially reacted, and unreacted droplets. The difference of these splat shapes strongly depends on the molten state of the particles at the moment of impact on the substrate. Thus, as explained before (Ref 6-9), during RPS nitriding of Al particles, the nitriding reaction starts during flight in the plasma, thereby the droplet contains molten (Al) and unmolten (AlN) phases before deposition. The relative amount of the molten Al and the formed nitride phase (in other words the nitridation degree) strongly affected the shape of the droplet during deposition.

As explained before in details (Ref 8), the nitriding reaction of Al particles starts after the melting of the particle. Thus, the Al particle surface is usually coated by an initial protective oxide film, as Rosenband and Gany explained before (Ref 23), which prevents good contact with the nitrogen gas and inhibits nitridation. When a metal melts, the initial protective oxide film is broken as a result of the tensile stress of increased volume. The nitrogen reacts intensely with the liquid metallic particles to form aluminum nitride and the nitriding reaction occurs via three steps and is summarized as follows:

- Surface nitriding of the particle with the formation of a crystalline nitride shell. Then due to the thermal stress of the large volume of molten Al, the Al starts to break the nitride shell to go or flow out. Moreover, in these

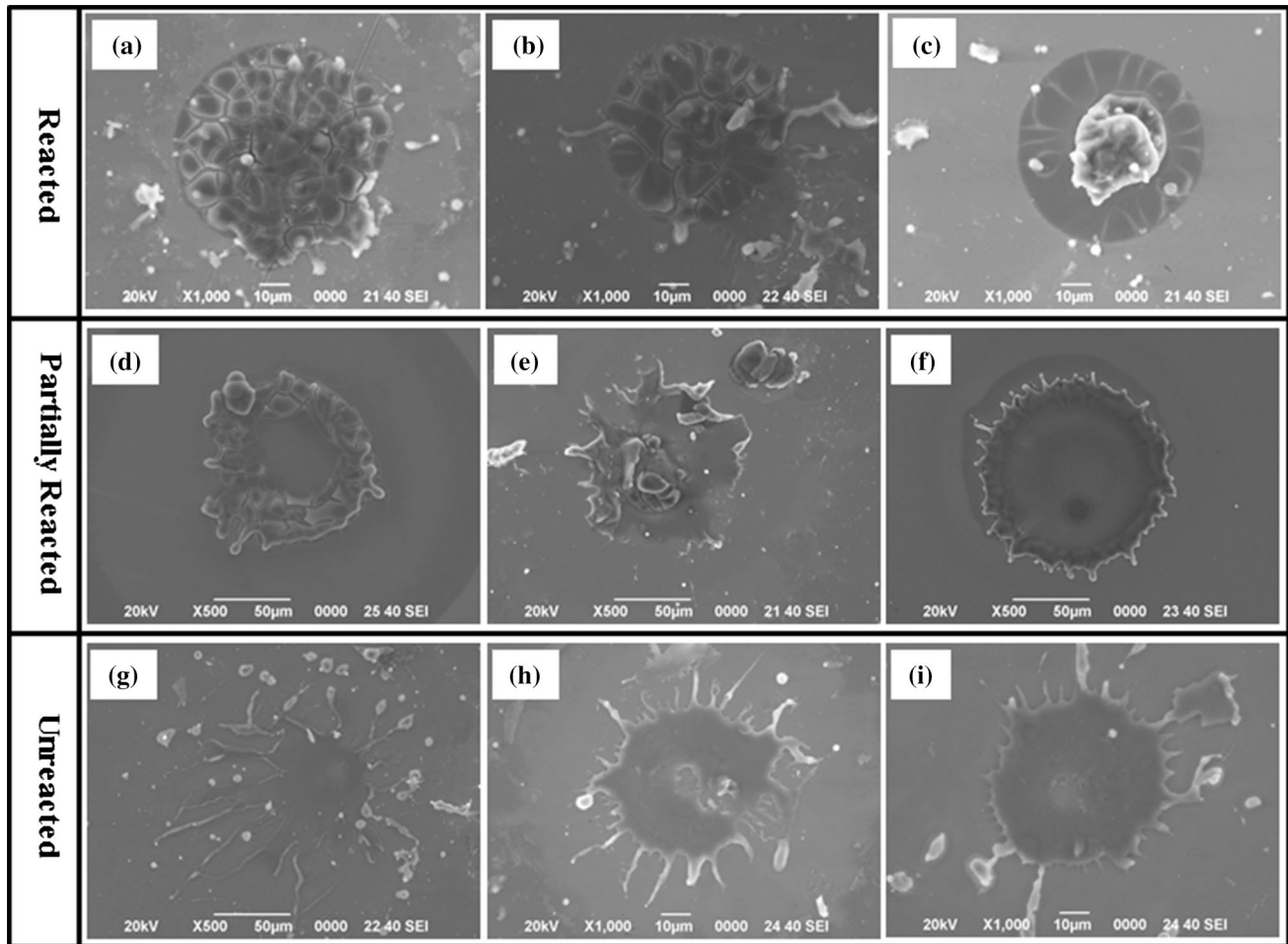


**Fig. 5** The morphology of the collected particles on mirror-polished SUS304 substrate in case of 30- $\mu\text{m}$  Al powders

high-temperature conditions, the generation rate of the reaction heat is enough to vaporize the molten Al present inside the shell and this is the beginning of the second step.

- The inner molten Al expands sufficiently enough to break the nitride shell and flow out as molten or vaporized Al core by a capillary-like phenomena.
- The diffused Al vapor reacted with the surrounding  $\text{N}_2$  through volume nitridation outside the shell with a remaining hole or an empty core.

This egg-shell is a characteristic feature for the formation of AlN through direct nitriding of Al powders, even when using large Al grains (Ref 24). The egg-shell and the nitriding mechanism were confirmed during reactive plasma spray nitriding of Al particles without using substrate in our previous studies (Ref 8). It is also worth mentioning that during spraying the collision of the particles on the substrate also assists the breakaway of the AlN shell and thereby the flow out of the molten Al phase.

Therefore, during the reactive plasma spraying of the Al particles in the  $\text{N}_2/\text{H}_2$  plasma, the particles may have

the following four deposition scenarios, which will control the splat shape:

- The particles finish the first nitriding step during flight (started the surface nitriding and formation of a crystalline nitride shell), and the second nitriding step will start during impact on the substrate. These droplets had an AlN surface (from the in-flight nitriding of aluminum particles) and an Al phase in the center. As AlN does not have a melting phase, the spherical shape of the solid aluminum nitride remained. However, the inside of the particle is in a molten or semi-molten Al phase at that time. When the droplet impacts on the substrate, the droplet surface collapses and the inside Al phase flows out. This molten Al will bond the droplet to the substrate. The splat shape of these droplets will strongly depend on the amount of molten Al phase in the center. In the case of a small Al amount, the particles tend to give a reacted disk splat shape as shown in Fig. 5(a) and (b). Thus, the small amount of Al is easily nitrided through plasma irradiation. On the other hand, in the case of a large amount of molten Al phase, the particles tend to form partially reacted splat with a nitride shell

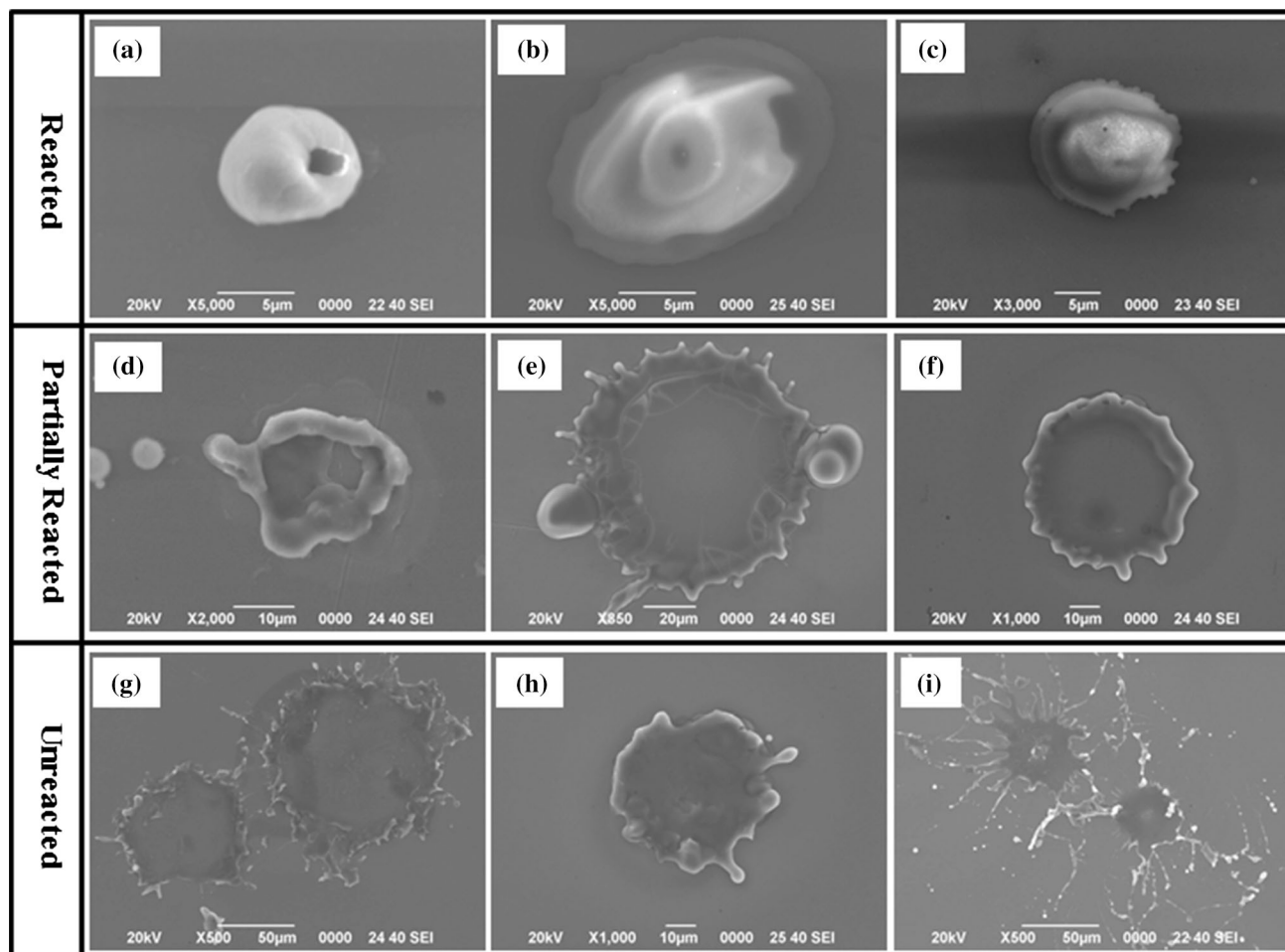


**Fig. 6** The morphology of the collected particles on mirror-polished SUS304 substrate in case of 15- $\mu\text{m}$  Al powders

outside and melted Al in the center of the splat as shown in Fig. 5 and 6(d)-(f).

- The particles finish the first nitriding step (surface nitriding) as well as the second step (breakaway or flow out of molten Al) during flight. The particles impacting on the substrate occurs during the third nitriding step. These particles tend to form the reacted egg-shell splat as shown in Fig. 5(c) and 6(a)-(c). These kinds of splats are more common in a case using fine particles.
- The particles complete the three reaction steps during flight (AlN completely forms during flight), these reacted droplets will never deposit on the substrate. Thus, AlN phase never deposits on the substrate (it does not have a molten state to deposit).
- The particles do not react with the surrounding nitriding phases and deposit as a molten Al phase. These particles tend to form mainly Al splash splats as shown in Fig. 5 and 6(g)-(i).

In addition, decreasing the particle size of the feedstock powder also affected the droplet deposition behavior as it affected the nitriding rate. Thus, decreasing the feedstock particle size improved the possibility of surface nitriding

and promoted the nitriding conversion through an increase in the specific surface area. Therefore, using the 15- $\mu\text{m}$  Al particles increased the nitriding area compared to 30- $\mu\text{m}$  Al particles, which enhanced the formation of AlN phase. Furthermore, the larger particles need eight times more heat to reach the same temperature than a particle with half the diameter as reported by Remesh et al. (Ref 25). Hence, the heat absorbed per unit volume is the inverse of the particle diameter. The large particle surface area (through which the heat is transferred) increases by four times compared to a particle with half its diameter. Furthermore, the particles melting and decomposition behavior was affected when decreasing the particle size. Thus, under the same temperature exposition, the small particles attain a higher temperature than the larger ones. Thereby, the heat conduction inside the small particles is faster and their decomposition rates are faster than for the large particles.

This leads to a shift of the droplet deposition behavior with decreasing the particle size. The reacted droplets mainly have the egg-shell-shaped splat as shown in Fig. 6(a)-(c). The partially reacted droplet showed a more uniform disk shape with a thicker nitride shell as shown in

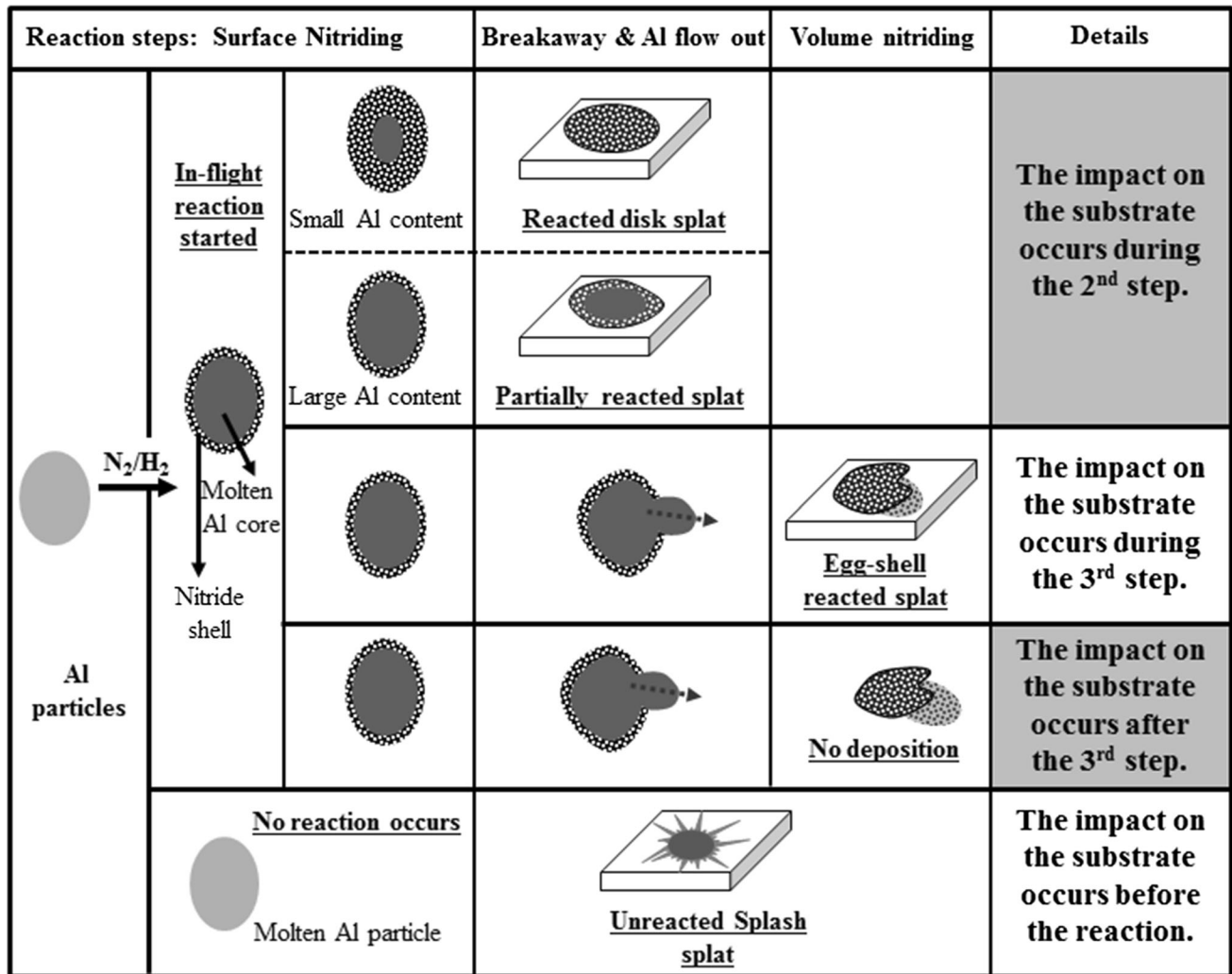


Fig. 7 Schematic expression of the splat formation during RPS nitriding process of Al particle

Fig. 6(d)-(f) compared to the larger Al in Fig. 5. The unreacted droplet tends to form splash splats with shorter splash fingers as shown in Fig. 6(g)-(i) compared to the larger Al particles in Fig. 5. Figure 7 schematically shows the splat formation mechanism during reactive plasma spray nitriding of Al particles. It is noteworthy that, in the RPS process, changing the particle velocity (i.e., with changing the spray system), particle collision energy (i.e., changing the particle size), and the reaction time (i.e., changing the spray distance) influences the splat shape and the ratio of each shape. Figure 8 shows the influence of the particle size and the spray distance on the ratio of the reacted, partially reacted, and unreacted splats. It is clear that, the number of reacted splats increased gradually with decreasing the particle size as well as increasing the spray distance. It is due to improving the nitriding reaction with decreasing the particle size and increasing the spray distance as explained before.

Herein, the splat morphology during reactive plasma nitriding of Al particles was investigated. The reacted ni-

tride content, the molten state content, and the time of droplet impacting on the substrate strongly control the splat shape. The collected splats were classified to reacted, partially reacted, and unreacted splats. Moreover, the particle size of the feedstock powder had a significant effect on the splat shapes during the RPS process.

### 3.2 Influence of Feeding Rate During Reactive Plasma Spraying Nitriding

The influence of the feeding rate during the RPS process was firstly investigated by increasing the carrier gas flow rate. However, increasing the carrier gas flow rate disturbs the plasma jet. In addition, using a low carrier gas flow rate is favorable for the reactive plasma spraying process to keep the particle in the center of the plasma. Moreover, using a low carrier gas flow rate avoids a wide particle distribution in the side parts of the jet and thereby avoids the oxidation as reported before (Ref 8). Moreover, Fauchais et al. reported that, the powder feeding and

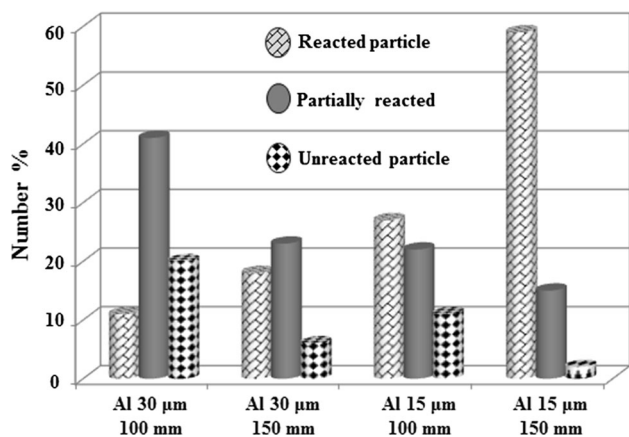


**Fig. 8** The ratio of the reacted, partially reacted, and unreacted particles using Al 30 and 15  $\mu\text{m}$  at 100 and 150 mm spray distances

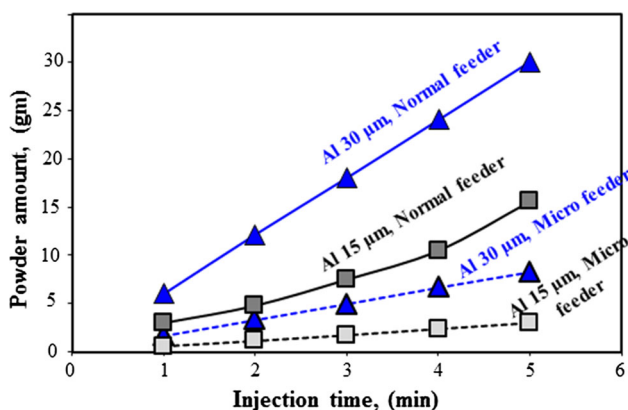


**Fig. 9** The injection rate of Al particles 30  $\mu\text{m}$  with using micro- and normal feeders using  $\text{N}_2$  carrier gas

flowability must be controlled to maintain the stability of the plasma and make the spray process consistent and reproducible (Ref 20-22).

Therefore, the effect of the powder feeding rate during the RPS of Al powder was investigated using a standard powder feeder under a low carrier gas flow rate (1 L/min of  $\text{N}_2$ : which was used in our previous studies (Ref 6-10)). The variation of the injection rate between the standard powder feeder (used in this part) and the micro-feeder (previous studies (Ref 6-10)), in the case of Al powders (30 and 15  $\mu\text{m}$ ) is shown in Fig. 9. It is clear that, the injection rate increased about five times when using the standard powder feeder for both powders under the same carrier gas flow rate.

Figure 10 shows the SEM cross-section microstructure of the fabricated coating in the case of Al 30  $\mu\text{m}$ . The coating thickness was about 1.3 mm which is thicker than the fabricated coatings seen in the case of the micro-feeder [about 80  $\mu\text{m}$  (Ref 6)]. Therefore, the coating thickness strongly improved by increasing the feeding rate. On the other hand, the nitriding reaction and phase composition are strongly affected by increasing the feeding rate

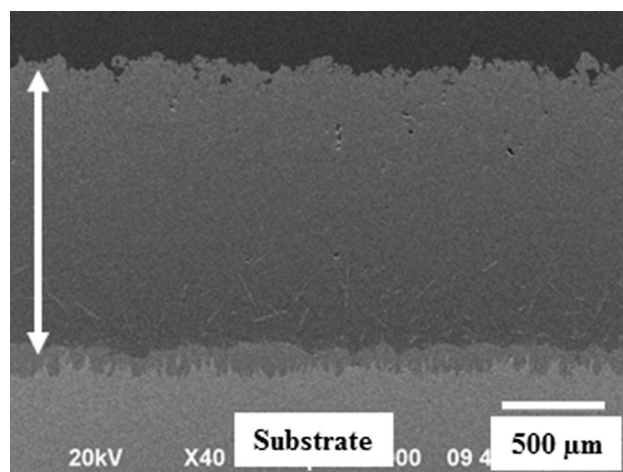


**Fig. 10** Cross-section microstructure of the fabricated coatings with increasing the feeding rate of 30- $\mu\text{m}$  Al powder at a 100 mm spray distance

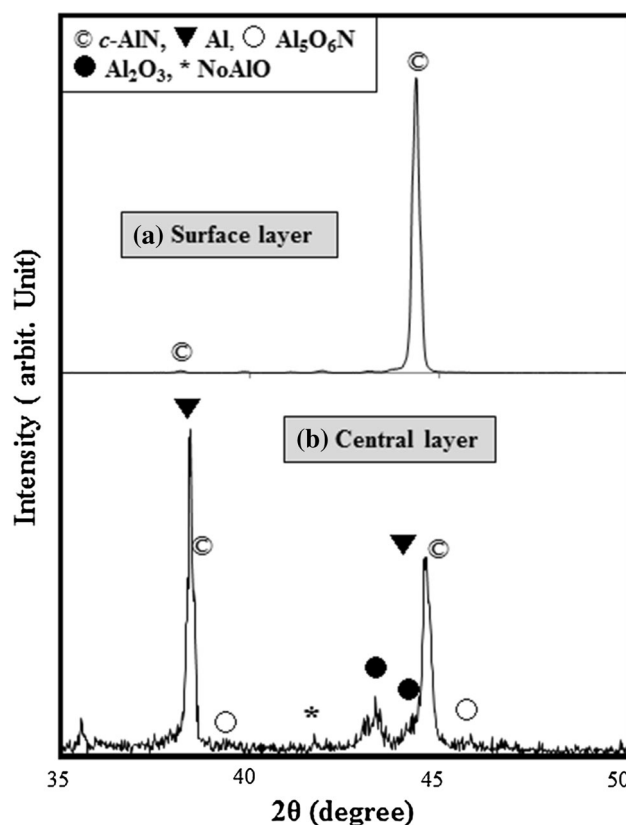


**Fig. 11** XRD spectra of the fabricated coatings using 30- $\mu\text{m}$  Al powder: (a) surface layers and (b) central layers after polishing 300  $\mu\text{m}$

as shown in Fig. 11. It is clear that, the outside surface layer (smooth surface: after fine polishing) consists of AlN phase, Fig. 11(a). However, the center layer (after removing about 300  $\mu\text{m}$  from the surface), consists of AlN/Al composite and some oxide phases like  $\text{Al}_2\text{O}_3$  and



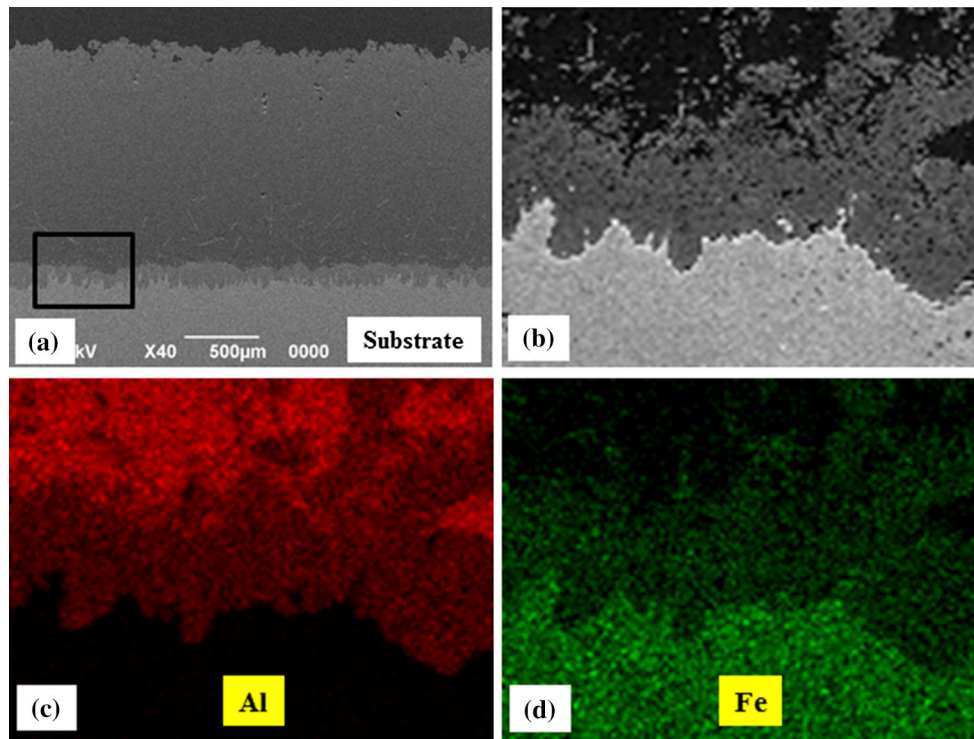


**Fig. 12** SEM cross-section of (a) the fabricated coating using only Al powder, (b) high magnification of the squared part in (a), (c) EDX image of Al, (d) EDX image of Fe

$\text{Al}_5\text{O}_6\text{N}$  as shown in Fig. 11(b). It reveals that, with increasing the powder feeding rate, the amount of the powders is high and not all of the particles completely reacted with the surrounding  $\text{N}_2/\text{H}_2$  plasma to give a pure AlN. On the other hand, the cross-section of the coating in Fig. 10 showed a thick layer ( $\sim 100\ \mu\text{m}$ ) between the substrate and the fabricated coating. It is an inter-metallic layer that was confirmed by the EDX analysis in Fig. 12. The formation of such an inter-metallic layer between the coating and the substrate is attributed to the interaction between the molten Al (unreacted Al) phase and the substrate surface. It indicated that some of Al metallic phase deposited as is without reaction with the  $\text{N}_2$  plasma, which agrees with the XRD result in Fig. 11.

As explained in details before (Ref 8), the nitriding reaction of the Al particles with the nitriding species in the plasma starts after the particle melting during flight. The nitriding occurs at the surfaces of these molten Al particles and forms nitride layers or shells surrounding the molten Al during flight. These partially reacted particles complete their reaction after deposition on the substrate through  $\text{N}_2$  plasma irradiation. However, with increasing the injection rate, the amount of the powders supplied to the plasma increased and not all particles can complete their reaction through the  $\text{N}_2$  plasma irradiation to give a pure AlN coating. Thus, with increasing the powder amount supplied to the plasma, the accelerated molten or semi-molten particles will easily coagulate together after colliding on the substrate. This will prevent

the  $\text{N}_2$  access to the entire of these particles in order to complete the nitriding reaction and form pure AlN. It is well known that, the aggregation of Al particles is the main problem for the fabrication of AlN powders through the direct nitriding of Al powders due to the low melting point of Al (933 K) (Ref 26-28). The surface layer completed its reaction after depositions on the substrate due to the  $\text{N}_2$  plasma irradiation and the lack of further particle deposition. Figure 13 schematically shows the nitriding mechanism of the Al particles with increasing the feeding rate.

It is concluded that increasing the powder injection rate in the case of Al  $30\ \mu\text{m}$  enhanced the coating thickness. However, the Al particles were not completely nitrided due to the coagulation and coalescing of the molten or semi-molten particles on the substrate. The fabricated coating consists of an inter-metallic layer, Al/AlN composite layers on the center, and AlN layers on the surface.

On the other hand, with increasing the injection rate of the Al  $15\ \mu\text{m}$  feedstock powder, it was possible to fabricate a  $500\text{-}\mu\text{m}$ -thick coating which is much thicker than the fabricated coatings using the micro-feeder for both of the Al powders. Figure 14 shows the cross-section microstructure of the fabricated coatings when increasing the feeding rate of the  $15\text{-}\mu\text{m}$  Al powder. Moreover, the microstructure of the center part of the coating is shown in Fig. 14(b), and the coatings contain pores which are well known in the reactive plasma spray process (Ref 4, 5). The fabricated coating mainly consists of AlN phase as shown

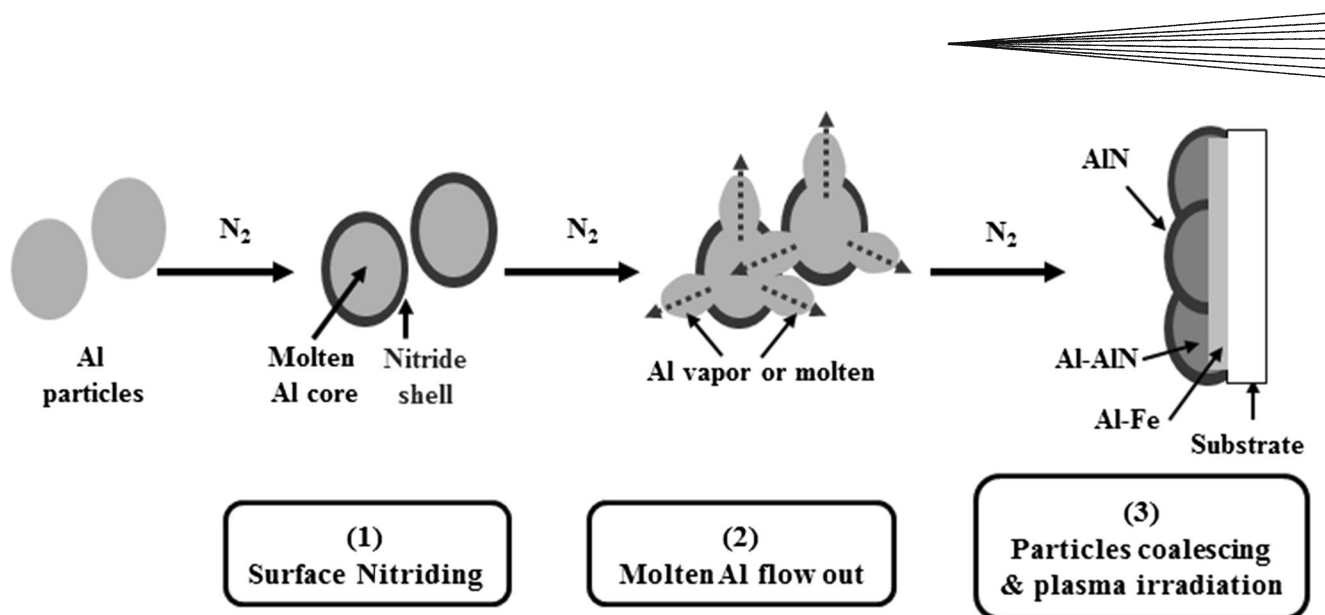


**Fig. 13** Schematic expression of the nitriding process of Al particle in APS process with increasing the powder feed rate

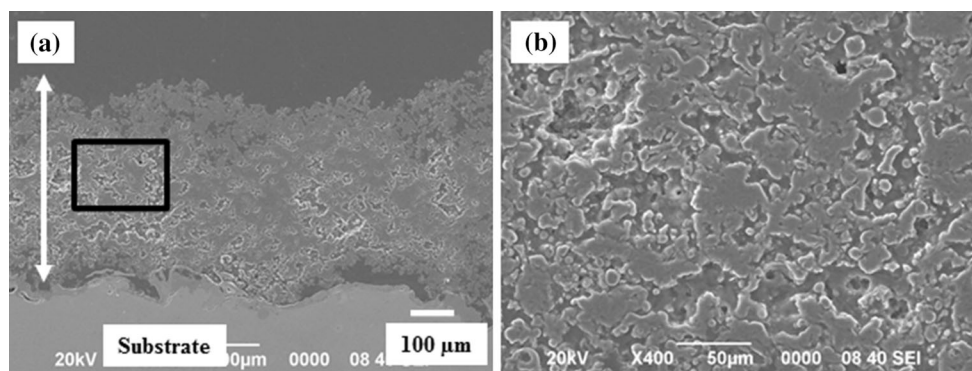


**Fig. 14** Cross-section microstructure of the fabricated coatings with increasing the feeding rate of 15- $\mu\text{m}$  Al powder at a 100 mm spray distance and (b) high magnification of the squared part in (a)

in the XRD spectra in Fig. 15. It is clear that both the surface and center layers (after removing about 200  $\mu\text{m}$  from the surface) consist of AlN phase. Therefore, with increasing the injection rate of the fine Al powders, it was possible to fabricate dense and thick AlN coatings.

Improving the nitriding reaction with decreasing the particle size is attributed to the increasing specific surface area (reacting area), which improves the possibility of surface nitriding. Therefore, after the 1st step of nitriding the amount of molten Al in the core decreased and is easy to completely flow out and nitride through volume nitriding. Furthermore, the particle size of feedstock powders also affects its melting behavior. Thus, the heat capacity of the small particles is smaller than that of the large particles, which makes the increase of its temperature faster than the large particles. Also, the total heat transfer to the small particles is larger than that to the larger particles at a constant weight. Therefore, the heat conduction inside the small particles is faster and its decomposition rates are higher than for large particles. Decreasing the coating thickness with decreasing the

particle size is attributed to the excessive vaporization of the fine Al particles during flight compared to the large particles, as explained in detail previously (Ref 8). It worth mentioning that the fabricated coating in case of 15  $\mu\text{m}$  slightly peeled from the substrate surface which is attributed to the thermal expansion difference between the fabricated ceramic coating and the metallic substrate. It is considered as a strong indication for the complete nitriding of Al powders and the formation of an AlN coating.

Herein, the influence of feeding rate was investigated during RPS of Al powders. In case of large particle size powder increasing the flow rate assisted the formation of thick AlN/Al composite coatings in the RPS process. The remaining Al phase is attributed to the easy coagulation and coalescing of the large Al particles on the substrate surface with increasing its amount. On the other hand, decreasing the particle size is a suitable solution to enhance nitriding conversion and to fabricate thick AlN coatings in the RPS process under an increased feeding rate.

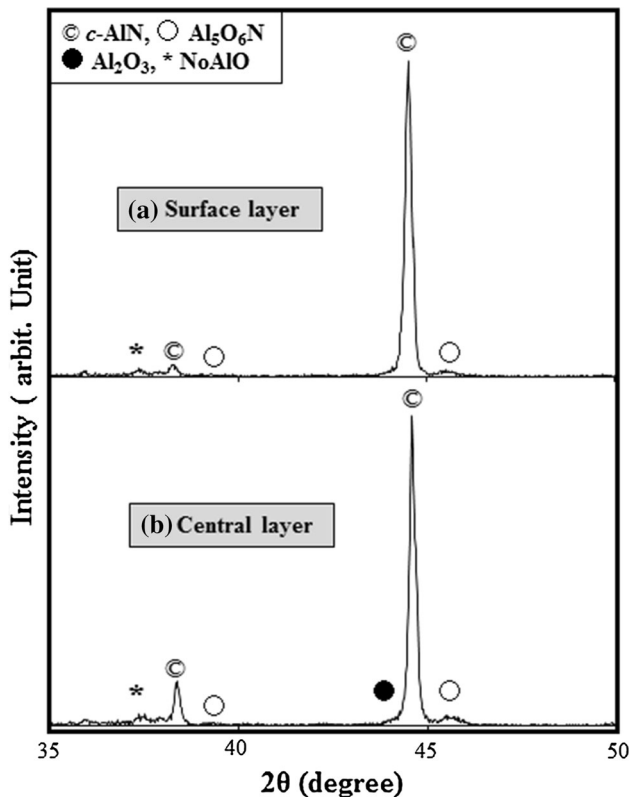


**Fig. 15** XRD spectra of the fabricated coatings using 15- $\mu\text{m}$  Al powder: (a) surface layers and (b) central layers after polishing 200  $\mu\text{m}$

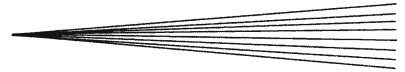
## 4. Conclusion

The splat morphology during reactive plasma spray nitriding of Al particles was clarified. By considering only the nitride phase formation, the splat morphology was divided into three groups: reacted, partially reacted, and unreacted splats. The splat formation is strongly related to the nitride content, the molten Al phase, and the time of the droplet impacting on the substrate surface. The splat formation is strongly affected by the reaction-related factors like particle size and spray distance due to its effect on the nitriding conversion and molten phase content.

On the other hand, the effect of the feedstock powder feeding rate was investigated during the RPS nitriding of Al powders. Increasing the feeding rate of the large Al particles assist the formation of thick AlN-Al composite coatings with AlN surface layers. It is attributed to the aggregation and coagulation of Al particles on the substrate surface, which prevent the complete nitriding through plasma irradiations. Decreasing the particle size improved the nitriding conversion and thereby avoiding Al particle coagulation. Thick AlN coatings of about 500  $\mu\text{m}$  were successfully fabricated using fine Al particles (15  $\mu\text{m}$ ) and increasing the feedstock feeding rate.

## References

1. H.O. Pierson, *Handbook of Refractory Carbides and Nitrides*, Noyes, New Jersey, USA, 1996, p 237-239
2. A.W. Wemer, *Carbide, Nitride and Boride Materials Synthesis and Processing*, Chapman & Hall, London, 1997, p 6-68
3. S. Nakamura, The Roles of Structural Imperfections in InGaN-Based Blue Light-Emitting Diodes and Laser Diodes, *Science*, 1998, **281**, p 956-961
4. M. Fukumoto, M. Yamada, T. Yasui, and K. Takahashi, Fabrication of Aluminum Nitride Coating by Reactive RF Plasma Spray Process, *Proc. International Thermal Spray Conference (ITSC)*, 2004, CD
5. M. Yamada, T. Yasui, M. Fukumoto, and K. Takahashi, Nitridation of Aluminum Particles and Formation Process of Aluminum Nitride Coatings by Reactive RF Plasma Spraying, *Thin Solid Films*, 2007, **515**(9), p 4166-4171
6. M. Shahien, M. Yamada, T. Yasui, and M. Fukumoto, Cubic Aluminum Nitride Coating Through Atmospheric Reactive Plasma Nitriding, *J. Therm. Spray Technol.*, 2010, **19**(3), p 635-641
7. M. Shahien, M. Yamada, T. Yasui, and M. Fukumoto, Fabrication of AlN Coatings by Reactive Atmospheric Plasma Spray Nitriding of Al Powders, *Mater. Trans.*, 2010, **51**(5), p 957-961
8. M. Shahien, M. Yamada, T. Yasui, and M. Fukumoto, Reactive Atmospheric Plasma Spraying of AlN Coatings: Influence of Aluminum Feedstock Particle Size, *J. Therm. Spray Technol.*, 2011, **20**(3), p 580-589
9. M. Shahien, M. Yamada, T. Yasui, and M. Fukumoto, Controlling of Nitriding Process on Reactive Plasma Spraying of Al Particles, *IOP Conference Series: Mater. Sci. Eng.*, 2011, **18**, 202006. doi: [10.1088/1757-899X/18/20/202006](https://doi.org/10.1088/1757-899X/18/20/202006)
10. M. Shahien, M. Yamada, T. Yasui, and M. Fukumoto, Influence of Plasma Gases on Fabrication of AlN Coatings Through Atmospheric Plasma Nitriding Process, *Ind. Appl. Plasma Process*, 2010, **3**, p 1-10
11. M. Shahien, M. Yamada, T. Yasui, and M. Fukumoto, Influence of  $\text{NH}_4\text{Cl}$  Powder Addition for Fabrication of Aluminum Nitride Coating in Reactive Atmospheric Plasma Spray Process, *J. Therm. Spray Technol.*, 2011, **20**(1-2), p 205-212
12. M. Shahien, M. Yamada, T. Yasui, and M. Fukumoto, In situ Fabrication of AlN Coating by Reactive Plasma Spraying of Al/AlN Powder, *Coatings*, 2011, **1-2**, p 88-107
13. M. Shahien, M. Yamada, T. Yasui, and M. Fukumoto, Synthesis of Cubic Aluminum Nitride Coating from  $\text{Al}_2\text{O}_3$  Powder in Reactive Plasma Spray Process, *Mater. Trans.*, 2013, **54**(2), p 207-214
14. M. Shahien, M. Yamada, T. Yasui, and M. Fukumoto,  $\text{N}_2$  and  $\text{H}_2$  Plasma Gases' Effects in Reactive Plasma Spraying of  $\text{Al}_2\text{O}_3$  Powder, *Surf. Coat. Technol.*, 2013, **216**, p 308-317
15. M. Shahien, M. Yamada, T. Yasui, and M. Fukumoto, Reactive Plasma Spraying of Fine  $\text{Al}_2\text{O}_3/\text{AlN}$  Feedstock Powder, *J. Therm. Spray Technol.*, 2013, **22**(8), p 1283-1293
16. M. Shahien, M. Yamada, T. Yasui, and M. Fukumoto, Reactive Plasma Sprayed Aluminum Nitride Based Coating Thermal Conductivity, *J. Therm. Spray Technol.*, 2015, **24**(8), p 1385-1398
17. P. Fauchais, M. Fukumoto, A. Vardelle, and M. Vrdelle, Knowledge Concerning Splat Formation: An Invited Review, *J. Therm. Spray Technol.*, 2004, **13**(3), p 337-360
18. M. Fukumoto, I. Ohgitani, and T. Yasui, Effect of Substrate Surface Change on Flattening Behaviour of Thermal Sprayed Particles, *Mater. Trans.*, 2004, **45**(6), p 1869-1873
19. M. Fukumoto, I. Ohgitani, Y. Tanaka, and E. Nishioka, Flattening Problem of Thermal Sprayed Particles, *Mater. Sci. Forum*, 2004, **449**(452), p 1309-1312
20. P. Fauchais, A. Vardelle, and B. Dussoubs, Quo Vadis Thermal Spraying?, *J. Therm. Spray Technol.*, 2001, **10**(1), p 44-66
21. P. Fauchais, G. Montavan, and G. Bertrand, Influence of Powders on Thermal Spray Coating Structures: Recent Developments in Nano or Finely Structured Coatings and Some Safety Issues, *Proc. International Thermal Spray Conference (ITSC)*, 2009, p 799-817



22. M. Vardelle, A. Vardelle, P. Fauchais, K.-I. Li, B. Dus-soubs, and N.J. Themelis, Controlling Particle Injection in Plasma Spraying, *J. Therm. Spray Technol.*, 2001, **10**(2), p 267-284
23. V. Rosenband and A. Gany, Activation of Combustion Synthesis of Aluminium Nitride Powder, *J. Mater. Process. Technol.*, 2004, **147**, p 179-203
24. T. Fujii, K. Yoshida, K. Suzuki, and S. Ito, Direct Nitriding of Large Grains of Aluminum with 2 mm Size, *Solid State Ionics*, 2001, **141-142**, p 593-598
25. K. Remesh, H.W. Ng, and S.C.M. Yu, Influence of Process Parameters on the Deposition Footprint in Plasma-Spray Coating, *J. Therm. Spray Technol.*, 2003, **12**, p 377-392
26. C. Lin and S. Chung, Combustion Synthesis of Aluminum Nitride Powder Using Additives, *J. Mater. Research*, 2001, **16**(8), p 2200-2208
27. Y. Qiu and L. Gao, Nitridation Reaction of Aluminium Powder in Flowing Ammonia, *J. Eur. Ceram. Soc.*, 2003, **23**, p 2015-2022
28. M. Radwan and M. Bahgat, A Modified Direct Nitridation Method for Formation of Nano-AlN Wiskers, *J. Mater. Process. Technol.*, 2007, **181**, p 99-105